The Morphological Study of a Novel Non-Chromate Coating on Galvanized Steel Sheet

CHING-KUO KUO

New Materials Research and Development Department
China Steel Corporation

Chromate conversion coatings with hexavalent chromium are currently being replaced by eco-friendly surface treatments due to environmental legislation.   A novel non-chromate passivating coating based on vanadium compound in an acidic system has been successfully synthesized.   This new coating for galvanized steel meets the general standards such as those for corrosion resistance, black tarnish resistance, and adherence.   The corrosion resistance of the new coating was evaluated by salt spray test and polarization curves.   The property of black tarnish resistance was improved by the addition of aluminum ion.   The distribution of the elemental composition of the new coating was studied by glow discharge spectrometer (GDS) and X-ray photoelectron spectroscopy (XPS) to investigate the microstructure.   The superiority of the new coating can be characterized by the following aspects: (a) vanadyl-phosphate complexes in the coating can enhance the barrier effect which suppresses diffusion of corrosive elements and improve corrosion resistance; and (b) P-O-Zn and Si-O-Zn bonds formed in the coating/zinc interface enhance the adherence of the coating.

1. INTRODUCTION

Conventionally, chromate conversion coatings with hexavalent chromium (Cr^{6+}) for galvanized steel sheets have been widely used as surface treatments such as passivations due to their excellent corrosion protection and low cost.   However, such chromate coatings are toxic and regulated by global environmental legislation, such as Waste Electrical and Electronic Equipment (WEEE)[1] and Restriction of Hazardous Substances (RoHS)[2]. As a result, a great deal of interest in developing non-chromate passivating coatings that do not contain hexavalent chromium attracts much attention today[3-5].

Improving corrosion protection is one of the ideas for developing non-chromate passivating coatings in light of the inferior corrosion resistance of these coatings. Improvement methods include: (1) barrier protection for the sacrificial zinc layer against corrosive elements (e.g. oxygen, water, and chlorine ions); and (2) inactivation of zinc surface or formation of hardly soluble compounds in the coating/zinc interface.

Furthermore, steel coils stored in higher temperature and humid environments may develop black tarnish defects on the surface.   Existence of these defects not only affects the commercial value and decorative appearance of products, but also decreases the adhesion between the coating film and the substrate.

In order to solve the above mentioned problems, this paper studies non-chromate solutions using various acidic solvents and additives in order to investigate the influence on corrosion resistance and black tarnish resistance.   In particular, the study pays attention to the relationship between the coating properties and the microstructure of the coating.

2. EXPERIMENTAL PROCEDURE

2.1 Experimental Methods

In the following study, aqueous non-chromate solutions were prepared in the laboratory with various acidic solvents that included vanadium salts and some additives, as listed in Table 1, which were coated on hot-dip galvanized steel sheets and baked up to 100 (Peak Metal Temperature ; PMT). These coating weights were controlled to about 0.2 g/m^2.

2.2 Analyzing Methods and Instruments

The properties of the coated specimens, including corrosion resistance and black tarnish resistance, were evaluated.   The corrosion resistance of the specimens was measured by salt spray tests (JIS Z2371).   The black tarnish resistance of the specimens was tested under 100% humidity, 50   , and 240 hours.

Table 1   Comparison of acidic solvents in novel non-chromate coatings

Sample No.	Major element components	Solvents
1	Vanadium, Silica, Oxygen	Phosphoric acid, and water
2	Vanadium, Silica, Oxygen	Formic acid, and water

Polarization curves of specimens were conducted in 3.5% $NaCl_{(aq)}$ solution with the use of platinum as the auxiliary electrode, and Ag/AgCl as the reference electrode. IR spectra were performed with a Varian 3600 Fourier-Transform IR spectrometer in the range of 400-4,000 cm^{-1}. Surface morphology and elemental analysis were observed with a JEOL 6300 scanning electron microscopy (SEM) and energy dispersive spectrometer (EDS). Depth profile and electron spectra were measured with electron spectroscopy for chemical analysis (ESCA; model: PHI-5000 VersaProbe**)**. Depth profile and elemental composition were analyzed with glow discharge spectrometer (GDS; model: RF GD Profiler HR).

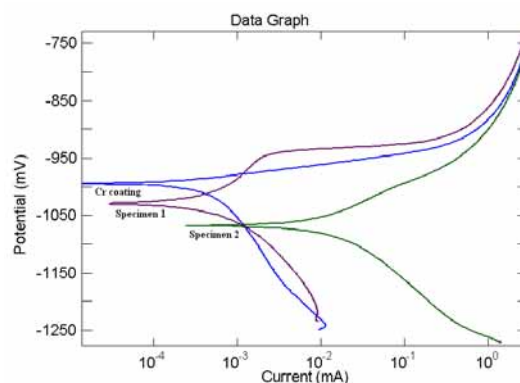## 3. RESULTS AND DISCUSSION

3.1 Corrosion Resistance

3.1.1 Salt Spray Test

The salt spray test (SST) is the standard method within the industry to evaluate the corrosion protection properties of a coating system. The testing method was designed to accelerate corrosion processes under wet conditions and the influence of electrolytes. It is an empirical method but widely accepted due to its relatively short testing times and the simplicity of the practical experiment.

Within 72 hours SST, the white rust region on the non-chromate coated galvanized steel sheets (specimen **1** and specimen **2**) do not exceed 10% of the total exposed area. It is clear that such non-chromate specimens show better corrosion resistance for various applications.

3.1.2 Electrochemical Property of Coatings

Polarization curves (specimens **1**, **2**, and Cr coating) are indicated from Fig. 1 to be measured in 3.5% $NaCl_{(aq)}$ solution. The data of polarization curves, where corrosion potential is denoted by $E_{corr.}$, corrosion current by $I_{corr.}$, anodic Tafel slope by β_a, and cathodic Tafel slope by β_c, are listed in Table 2.

Fig. 1. Polarization curves of various specimens in the 3.5% $NaCl_{(aq)}$ solution.

Corrosion potential ($E_{corr.}$) of specimens from low to high: specimen **2** (-1,068.4 mV) < specimen **1** (-1,029.3 mV) < Cr coating (-994.2 mV). Corrosion current ($I_{corr.}$) of specimens from low to high: Cr coating (0.052 mA/cm^2) < specimen **1** (0.076 mA/cm^2) < specimen **2** (0.098 mA/cm^2). Though the passivation of specimen **1** is worse than that of the Cr coating, the passivation of specimen **1** is still better than that of specimen **2**. The electrochemical result is consistent with the result of SST.

Comparison between specimen **1** and Cr coating: Tafel slopes (β_a and β_c) of Cr coating show that the corrosion resistance of Cr coating is attributed to the inhibition of the cathodic corrosion process. Although the specific passivating path of specimen **1** is not apparently observed from the Tafel slopes, the corrosion rate of zinc is still suppressed and the inhibition of corrosion is achieved.
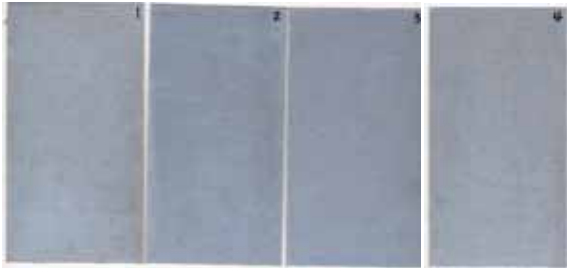
3.2 Black Tarnish Resistance

3.2.1 Specimen **1**

The surface condition of specimen **1** changes with the addition of aluminum ion after the black tarnish test. Tiny precipitation eluted on specimen 1 without
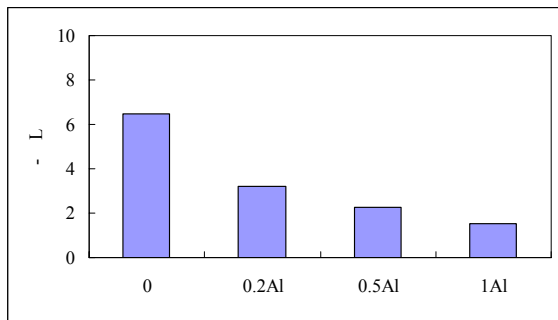
Table 2   Data of polarization curves for various specimens.

	$E_{corr.}$ (mV)	$I_{corr.}$ (mA/cm^2)	β_a (mV)	β_c (mV)
Specimen **1**	-1,029.3	0.076	46.319	56.938
Specimen **2**	-1,068.4	0.098	61.084	91.551
Cr coating	-994.2	0.052	18.241	172.240

aluminum ion resulted in a worse surface quality, as shown in Fig. 2. Surface quality became better upon aluminum ion being added (compared with no aluminum ion being added). The color difference (L) of the surface also became less pronounced upon aluminum ion being added (Fig. 3).

Fig. 2. Results of specimen **1** with various amounts of aluminum ion after black tarnish test; from left to right: 0.2, 0.5, 1, and 0 mole aluminum ion.
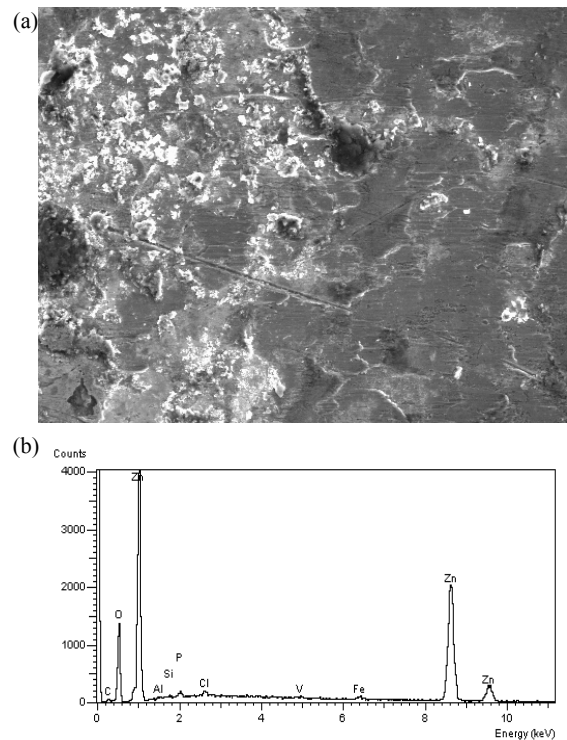

Fig. 3. Color difference (L) of surface with various amount of aluminum ion.
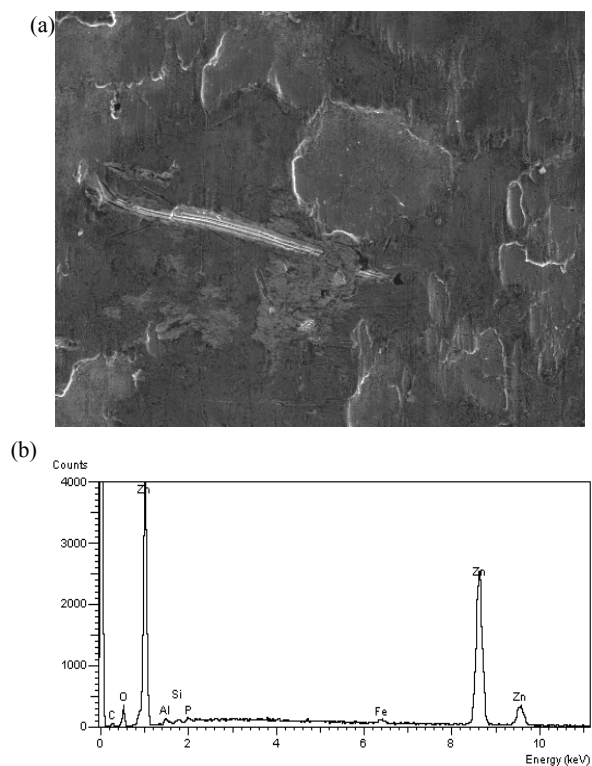
The tiny precipitation described above was further observed by SEM/EDS (see Fig. 4). Morphology showed that the impurity covering the surface was zinc corrosive (identified by EDS). No precipitation appeared after aluminum ion being added (see Fig. 5 and Fig. 6). Fig. 5 and Fig. 6 indicate that the morphology of the surface made from the skin-pass process is clear, and the weaker oxygen element intensity is detected by EDS. Consequently, the corrosion of zinc was inhibited effectively by adding aluminum ion in the humid environment.
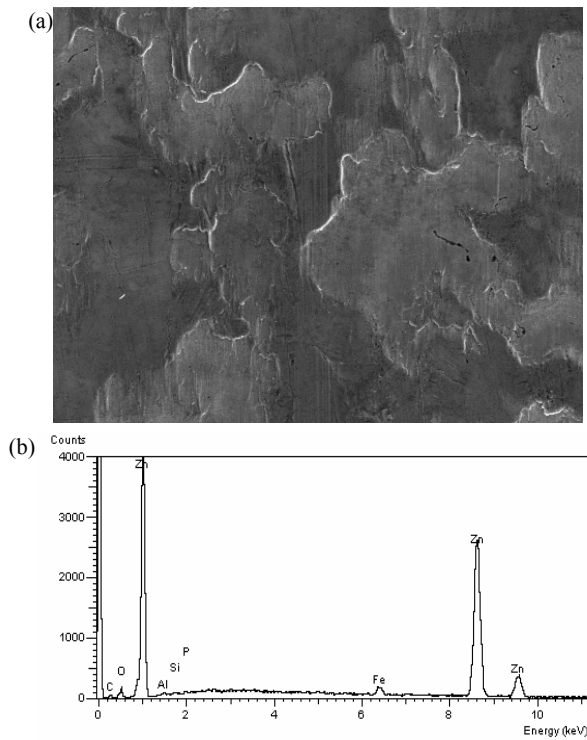
3.2.2 Specimen **2**

The surface of specimen **2** was covered with a white dust after the black tarnish test (see Fig. 7). The white dust identified by X-ray fluorescence spectroscopy (XRF) was zinc corrosive. The dust still appears when the concentration of formic acid is decreased. It is assumed that a zinc formate complex is formed from a chemical reaction between the specimen **2** solution and the zinc layer. However, a water soluble complex dissolves in the high humid environment, resulting in an accelerated corrosion process.

Fig. 4. (a) SEM morphology of specimen **1** without aluminum ion; and (b) EDS results of the surface.

Fig. 5. (a) SEM morphology of specimen **1** with 0.2 mole aluminum ion; and (b) EDS results of the surface.

Fig. 6. (a) SEM morphology of specimen **1** with 0.5 mole aluminum ion; and (b) EDS results of the surface.
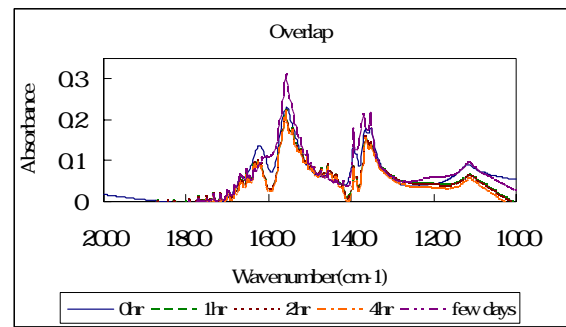

Fig. 7. Results of specimen **2** with various concentration of formic acid after black tarnish test; concentration of formic acid from left to right: 12.5, 25, and 50%.

Besides, formic acid has not been evaporated thoroughly during the drying process, which results in finger prints on the coating film. IR spectra of specimen **2** at various time intervals are shown in Fig. 8. The IR spectra of specimen **2** displays a characteristic band at 1,620 cm^{-1} corresponding to the C=O stretching frequency (contributed by formic acid). The characteristic band almost disappeared few days later. This band is ascribed to the residual solvent evaporating from the coating film.
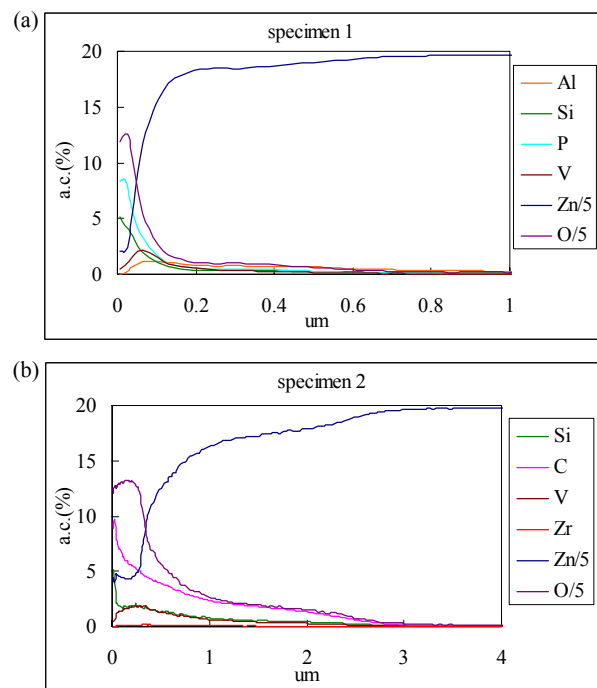
3.3 Distribution of Elemental Composition Within Non-chromate Coating

3.3.1 Glow Discharge Spectrometer

Fig. 8. FT-IR spectra of specimen **2** at various time intervals.

Glow Discharge Spectrometer (GDS) was applied in bulk analysis and depth profile of materials. Fig. 9(a) and Fig. 9(b) show the results for specimen **1** and specimen **2**, respectively. Fig. 9(a) demonstrates that the thickness of a coating film composed of Al, Si, P, V, O elements is about 0.1-0.2 μm. Atomic concentration of zinc increases from 91.33 to 95.11% as the depth reaches 0.2 to 0.5 μm. Atomic concentration of oxygen and phosphorus decreases from 5.27 to 2.94% and 0.55 to 0.27% accordingly. It is assumed that a chemical reaction between phosphoric acid and zinc layer results in the formation of oxo-complexes in the interface.

Fig. 9. GDS results of non-chromate coated GI sheets: (a) specimen **1**; and (b) specimen **2**.

From Fig. 9(b) it appears that the thickness of a coating film composed of Si, V, Zr, O, C elements is about 1 μm. Atomic concentration of zinc increases from 81.99 to 98.04% as the depth reaches 1 to 3 μm.

Atomic concentration of oxygen and carbon decreases from 12.92 to 1.33% and 2.33 to 0.17% accordingly. It is assumed that the corrosion resistance is contributed by the thicker coating film in comparison with that of specimen **1**. The reason for worse black tarnish resistance of specimen **2** is that zinc formate complex is formed by a reaction of formic acid and zinc layer. The zinc formate complex is dissolved in the humid environment and results in corrosion.

3.3.2 X-ray Photoelectron Spectroscopy

X-ray Photoelectron Spectroscopy (XPS) was applied in the analysis of elemental composition and its chemical valence. Depth profile of XPS could be achieved by Ar^+ ion sputtering. Table 3 lists the data of specimen **1** and correlated references[4-6]. Fig. 10 shows that the intensity of O element decreases upon inner layer. As shown in Fig. 11(a), two peaks, which are 531.2 eV (86%) and 532.9 eV (14%), respectively, appear at the simulation diagram of the 1st layer. Vanadyl- phosphate complexes such as $[V_2O_2(P_2O_7)]$ are presumed at the lower binding energy, whereas oxides of phosphorus or silica are presumed at the higher binding energy. The simulation diagram of the 5th layer shows that these two peaks still appear (Fig. 11(b)). However, the distribution of compounds changes with the different depths of coating film. The above results summarize that major vanadyl-phosphate complexes exist on the upper coating film, accompanying with minor oxides of phosphorus or silica. Major oxides of phosphorus or silica exist in the coating/zinc interface.

The V element which exists in the upper layer is shown in Fig. 12. In the simulation diagram of the 1st layer there appears only one peak (516.1 eV), which corresponds to V(IV)-P complex, as shown in Fig. 13(a). The simulation diagram of the 5th layer is similar to that of the 1st layer (Fig. 13(b)). This similarity means that no red-ox reaction happened in vanadium ion, and the composition of V(IV)-P complex remained intact at the different depths of coating film.
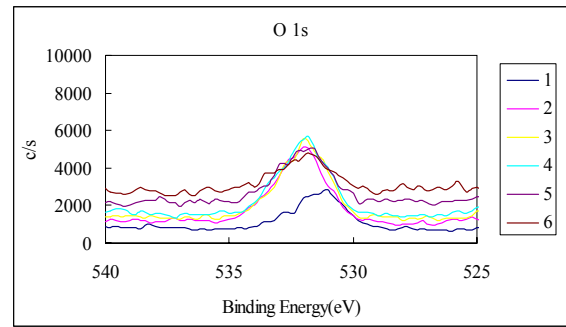

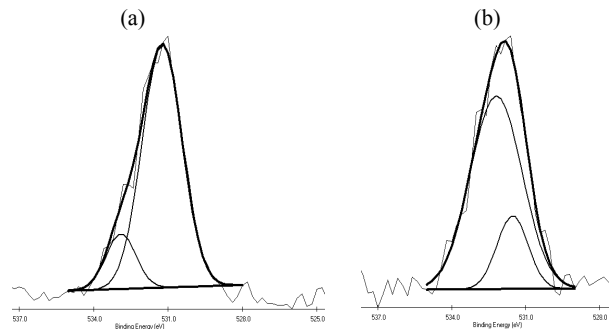**Fig. 10.** O-1s XPS spectra of specimen **1**.

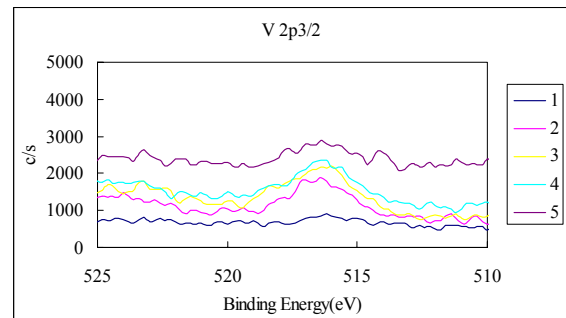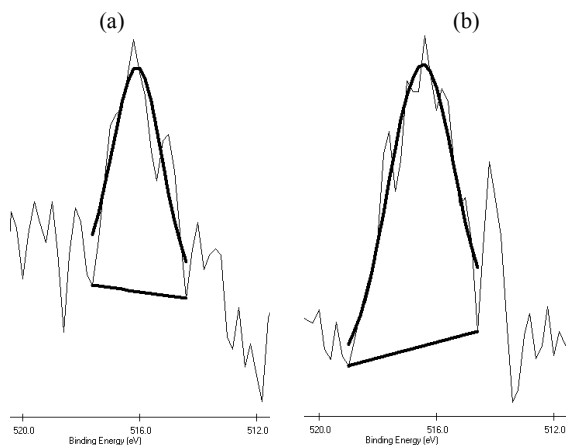**Fig. 11.** Simulation diagram of O-1s XPS spectra of specimen **1**: (a) the 1st layer; and (b) the 5th layer.
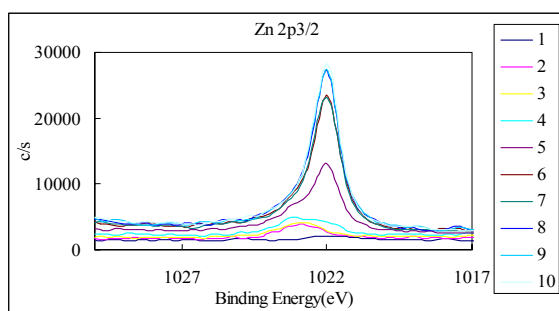

Fig. 12. V-2p XPS spectra of specimen **1**.

Table 3   XPS data of specimen 1 and correlated references[6-15]

	O-1s (eV)		V-2$p_{3/2}$ (eV)	Zn-2$p_{3/2}$ (eV)	
$V_2O_2(P_2O_7)$[6]	531.3		516.9	-	
P_2O_5[7-8]	532.2-534.3		-	-	
SiO_2[9-10]	532.1-534.3		-	-	
VO_2[11-12]	530.0-530.4		516.3	-	
V_2O_5[13-14]	530.3		516.6-517.7		
Zn[15]	-		-	1,021.6-1,022.1	
ZnO[16-18]	529.9-530.9		-	1,021.5-1,022.5	
$Zn(OH)_2$[15]	-		-	1,022.7	
Initial sputter	531.2(86%) (1st layer)	532.9(14%)	516.1 (1st layer)	1,022.8 (2nd layer)	
Final sputter (5th layer)	531.5(19%)	532.2(81%)	516.5	1,021.9(32%)	1,022.5(68%)

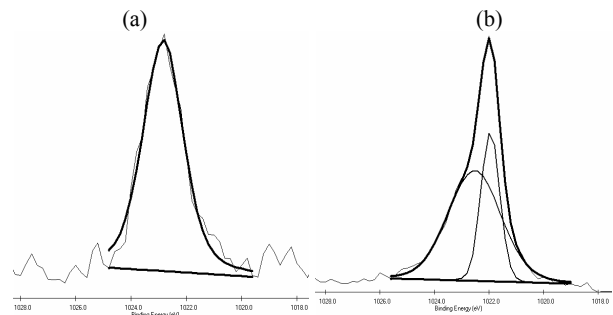**Fig. 13.** Simulation diagram of V-2p XPS spectra of specimen **1**: (a) the 1st layer; and (b) the 5th layer.

Fig. 14 shows that the intensity of the Zn element increases upon the inner layer. As shown in Fig. 15(a), the simulation diagram of the 2nd layer exhibits only one peak (1,022.8 eV), which corresponds to Zn^{2+} ion (Binding Energy of the peak is higher than that of ZnO). Zn element measured in the upper layer is attributed to the thinner coating layer and the higher roughness of the zinc layer. Furthermore, interfacial interaction between the non-chromate solution and the zinc layer promotes oxidation of zinc and the formation of bonding (P-O-Zn, Si-O-Zn bond), thus enhancing adhesion between the coating film and the zinc layer. As shown in Fig. 15(b), two peaks, which are 1,021.9 eV (32%) and 1,022.5 eV (68%), respectively, appear in the simulation diagram of the 5th layer. The second peak is ascribed to the neutral zinc increasing with depth, whereas the partially oxidized Zn^{2+} ions exist in the coating/zinc interface with the lower roughness.
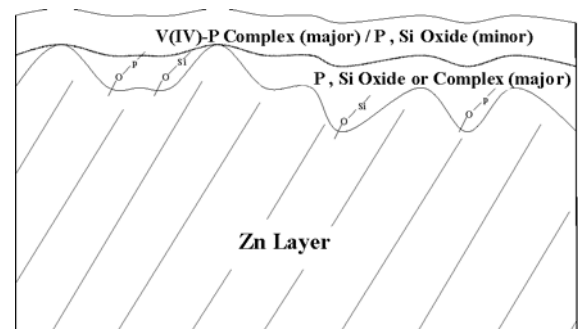

Fig. 14. Zn-2p XPS spectra of specimen **1**.

The schematic view of the composition of specimen **1**, as illustrated in Fig. 16, can be reasonably deduced from an analysis of GDS and XPS data (ignoring the existence of minor aluminum ion). Major V(IV)-P complexes exist in the upper film, accompanied by minor oxides of phosphorus, and silica, thus enhancing the barrier effect which suppresses the diffusion of cor-

rosive elements and improving the corrosion resistance; meanwhile, P-O-Zn and Si-O-Zn bonds formed in the coating/zinc interface enhance the adherence of the coating.

Fig. 15. Simulation diagram of Zn-2p XPS spectra of specimen **1**: (a) the 2nd layer; and (b) the 5th layer.

Fig. 16. Scheme of coating composition of specimen **1**.

4. CONCLUSIONS

(1) The phosphoric acid-based non-chromate coating, consisting of quantitative vanadium, phosphorus, silica, and aluminum ions, on galvanized steel sheets can meet the requirement of corrosion resistance with a specification of less than 10% white rust area ratio by 72 hours salt spray test.

(2) Electrochemical results showed that though passivation of phosphoric acid-based coating was worse than that of chromate coating, it was still better than that of formic acid-based coating. The result is consistent with the result of the salt spray test.

(3) Aluminum ions added in the phosphoric acid-based coating improved the property of black tarnish resistance and suppressed the elution of zinc corrosive.

(4) The microstructure of the novel non-chromate coating can be characterized by the following aspects: (a) vanadyl-phosphate complexes in the coating enhance the barrier effect which suppresses the diffusion of corrosive elements and improve the corrosion resistance; and (b) P-O-Zn and Si-O-Zn bonds formed in the coating/zinc interface enhance the adherence of the coating.

(5) A newly-developed non-chromate passivating coating based on vanadium compound in an acidic system has been successfully synthesized. This coating for galvanized steel meets the general standards such as those for corrosion resistance, black tarnish resistance, and adherence.

REFERENCES

1. The European Parliament and the Council of the European Union: Official Journal of the European Communities, 2003, L37/24.

2. The European Parliament and the Council of the European Union: Official Journal of the European Communities, 2003, L37/19.

3. JP PATENT 2002-214579, 2002, JFE.

4. JP PATENT 2006-005537, 2006, HSK.

5. JP PATENT 2007-238976, 2007, NIHON PARKERIZING.

6. T. P. Moser and G. L. Schrader, J. Catal., 1987, vol. 104, p. 99.

7. V. I. Nefedov, D. Gati, B. F. Dzhurinskii, N. P. Sergushin, and Y. V. Salyn, Zh. Neorg. Khimii, 1975, vol. 20, p. 2307.

8. R. Gresch, W. Mueller-Warmuth, and H. Dutz, J. Non-Cryst. Solids, 1979, vol. 34, p. 127.

9. D. Sprenger, H. Bach, W. Meisel, and P. Gutlich, J. Non-Cryst. Solids, 1990, vol. 126, p. 111.

10. K. Kishi and S. Ikeda, Bull. Chem. Soc. Jpn., 1973, vol. 46, p. 341.

11. J. Kasperkiewicz, J. A. Kovacich, D. Lichtman, J. Electron Spectrosc. Relat. Phenom., 1983, vol. 32, p. 128.

12. R. J. Colton, A. M. Guzman, J. W. Rabalais, J. Appl. Phys., 1978, vol. 49, p. 409.

13. R. Larsson, B. Folkesson, and G. Schoen, Chem. Scr., 1973, vol. 3, p. 88.

14. V. I. Nefedov, M. N. Firsov, and I. S. Shaplygin, J. Electron Spectrosc. Relat. Phenom., 1982, vol. 26, p. 65.

15. L. S. Dake, D. R. Baer, and J. M. Zachara, Surf. Interface Anal., 1989, vol. 14, p. 71.

16. J. Haber, J. Stoch, and L. Ungier, J. Electron Spectrosc. Relat. Phenom., 1976, vol. 9, p. 459.

17. D. W. Langer and C. J. Vesely, Phys. Rev. B, 1970, vol. 2, p. 4885.

18. S. W. Gaarenstroom and N. Winograd, J. Chem. Phys., 1977, vol. 67, p. 3500.